Front. Optoelectron. 2019, 12(3): 286–295
https://doi.org/10.1007/s12200-019-0864-y

RESEARCH ARTICLE

Nano-film aluminum-gold for ultra-high dynamic-range surface plasmon resonance chemical sensor

Briliant Adhi PRABOWO (✉)[1,2,3], I Dewa Putu HERMIDA[1], Robeth Viktoria MANURUNG[1], Agnes PURWIDYANTRI[3,4], Kou-Chen LIU (✉)[2,3,5,6]

1 Research Center for Electronics and Telecommunications, Indonesian Institute of Sciences, Bandung 40135, Indonesia
2 Department of Electronics Engineering, Chang Gung University, Taoyuan 33302, Taiwan, China
3 Biosensor Group, Chang Gung University, Taoyuan 33302, Taiwan, China
4 Research Unit for Clean Technology, Indonesian Institute of Sciences, Bandung 40135, Indonesia
5 Division of Pediatric Infectious Disease, Department of Pediatrics, Chang Gung Memorial Hospital, Taoyuan 33305, Taiwan, China
6 Department of Materials Engineering, Ming Chi University of Technology, New Taipei City 24301, Taiwan, China

Abstract An analytical and experimental study of nano-film aluminum (Al) for ultra-high dynamic range surface plasmon resonance (SPR) biosensor is presented in this article. A thin film of 16 nm Al is proposed for metallic sensing layer for SPR sensor. For the protective layer, a 10 nm of gold (Au) layer was configured on top of Al as a protection layer. This ultra-high dynamic range of SPR biosensor reached the bulk refractive index sample limit up to 1.45 RIU. For the analytical study, with the assumption of anisotropic refractive indices experiment, the dynamic range showed a refractive index value of around 1.58 RIU. The refractive index value limit achieved by the proposed sensing design is potentially implemented in various applications, such as in chemical detection and environmental monitoring study with high refractive index solution sample. The experimental results are presented as a proof-of-concept of the proposed idea.

Keywords dynamic range, surface plasmon resonance (SPR), sensor, aluminum (Al), gold

1 Introduction

Surface plasmon resonance (SPR) has emerged as one of the eminent biochemical sensor platforms gaining tremendous attention from scientists in recent decades [1,2]. Numerous potential applications in environmental monitoring, biomedical detection, and food science have been reported to employ and explore the distinctive features of SPR sensor, such as its high sensitivity, real-time and label-free detection [3–6]. The surface plasmon phenomena exist due to significant numbers of free electron confinement in the nanoscale thickness of metal film surface interfacing with the dielectric medium, such as water or air. The free electron oscillation in nanoscale can be observed by p-polarized light coupling through high refractive index prism, in particular, incident angle. In the resonance condition, the fraction energy of p-polarized light will be absorbed by the surface plasmon wave and results in a dark band in the reflectivity profile [7]. Interestingly, the reflectivity profile will be shifted to the lower or higher angle of incident light with the fluctuation of the refractive index medium value [8–10].

In chemo-sensor technology development, several researchers attempt to improve the sensitivity as optimized as possible along with the smallest limit of detection (LOD) for ultra-low concentration detection. This parameter of sensing performance plays an essential role in early diagnosis or in general experimental laboratory works requiring a small volume of sample with low concentration contained. Therefore, myriads of strategies were applied to improve the low concentration detection using nanosensing platform. Nevertheless, while efforts have been made constantly to achieve the lower LOD, another important sensing parameter such as dynamic range is not adequately explored in biosensing technology development.

In some particular applications, such as, in cancer marker early detection [11], diseases diagnosis [12], food contamination [13] and heavy metal detection [14], the sensitive and low detection limit performance in a

Received August 2, 2018; accepted October 29, 2018

E-mails: briliant.adhi.prabowo@lipi.go.id, jacobliu@mail.cgu.edu.tw

constructed sensor is critically required. Pertaining to the key roles of the sensitivity and low LOD, a variety of techniques have been proposed in the SPR sensor fabrication including the application of nanomaterial structures [15–17], 2D materials [18–21], advance grating structures [22] and novel metal film structures [23–26].

On the other hand, in several particular detection setups, high dynamic range performance is necessary, for instance in bio-detection involving high refractive index solution such as Dulbecco's modified eagle medium (DMEM) [6,27], or environmental monitoring for oil, toluene, or benzene contamination [28]. However, the trade-off between sensitivity/detection limit and dynamic range performance is a challenging factor for sensor designers [29–31]. A dynamic range refers to the targeted concentration range which can be detected by a sensing platform [32]. Typically, a platform with ultra-low LOD exhibits a very low dynamic range due to the low saturation point of the detection. In contrast, platforms with high dynamic range sensing usually suffer from the low sensitivity performance. Mishra et al. proposed a GaP-based Kretschmann prism for the SPR sensor to boost the dynamic range performance [33]. However, the GaP prism cost and availability in the market are disadvantageous factors for this purpose.

In SPR sensor, a thin film gold layer is applied as conventional metallic sensing layer owing to its stability and non-reactive behavior in the ambient environment [34,35]. Besides, the gold dielectric constant value is quite superior to enhance the plasmonic activity. Whereas, silver is also regarded potential as sensing layer due to its higher optical reinforcement to generate plasmonic fields than gold, yet, several drawbacks, such as toxicity issues and oxidation reactivity have made Ag less preferred in SPR sensor development [36]. Bimetallic and multilayer Ag/Au have also been exploited as an alternative sensing layer in SPR sensor configuration demonstrated in a portable platform by our group [23,24,37]. Using these noble metal sensing layer, the performance of the dynamic range is limited, particularly, in angular interrogation-based SPR sensor.

Another metal holding a potency to generate plasmonic field is Al. Previous studies reported the structural sensing configuration of Al film for the adhesion layer of the SPR metallic sensing layer [23,24]. Still, only few studies reported the application of Al for SPR biosensor configuration because of its limitation and the stability issues [38,39]. First, Al is reactive in oxidation and has the tendency to form an Al_2O_3 thin layer in the surface when it is exposed to ambient environment. Second, Al is reactive in the fluidic sample with acidic pH and thus, make it difficult when applied in several biomedical applications where the pH solution is present in major procedure such as the pH solution, such as acetate (pH 5.0) for facilitating surface chemistry and thiol activation [40]. Hence, a pure Al sensing layer is not feasible for practical use of SPR sensor applications; although, in theory, the pure Al has potential optical characteristics to trigger further dynamic range of SPR sensing platform and offers the benefit of low-cost material in comparison with the noble metals, such as gold and silver.

In this article, we proposed an Al film sensing layer protected by thin film gold in angular interrogation-based SPR sensor for ultra-high dynamic range performance and studied the numerical and analytical study. The experimental results are presented as a proof-of-concept of the proposed idea. The application of Al for the first layer of the sensing metal has shown the advantages over the use of a typical adhesion layer such as chromium (Cr). An analytical approach to this study was simulated and compared to the other sensing structures for the references [23,24]. It is found that by using the proposed SPR sensing layers, a dynamic range up to 1.45 RIU solution was successfully achieved. This high value of bulk refractive index solution is comparable to the 63.5 wt% of sucrose water concentration and 22% benzene on methanol solution.

2 Materials and methods

2.1 Simulation setup

The simulation setup was constructed by Kretschmann configuration of SPR sensor using an angular interrogation method. The optical parameters of the materials in this study were obtained from the published articles. The real and imaginary part of the dielectric constant (ε_R, ε_i), refractive indices (n) and extinction coefficient (k) parameters of Al and Au were obtained from the report of McPeak et al. [41], respectively. Subsequently, the optical parameters of H_2O as the reference medium were obtained from the article published by Hale and Querry [42]. The n and k of BK7 glass as the Kretschmann prism were obtained from Schott™ optical glass datasheet; while the shape of half cylindrical prism was taken into account. The utilization of the half cylindrical prism instead of the triangle or trapezoid prism was preferred to omit the refraction variable in the incident angle interface between free space and the prism. For the anisotropic refractive indices analysis, the assumption of 60 nm thickness for the refractive index value in the sensing surface was applied considering the surface chemistry of the thiol length (6 to 8 nm), the IgG protein size of around 13.7 nm [43] in some in biomedical applications and the target size such as viral particles of approximately 40 nm [6]. In this study, an SPR configuration approach using angular interrogation method in Kretschmann coupler configuration and red monochromatic wavelength of 600 nm was utilized. The simulation description of the experimental setup is demonstrated in Fig. 1.

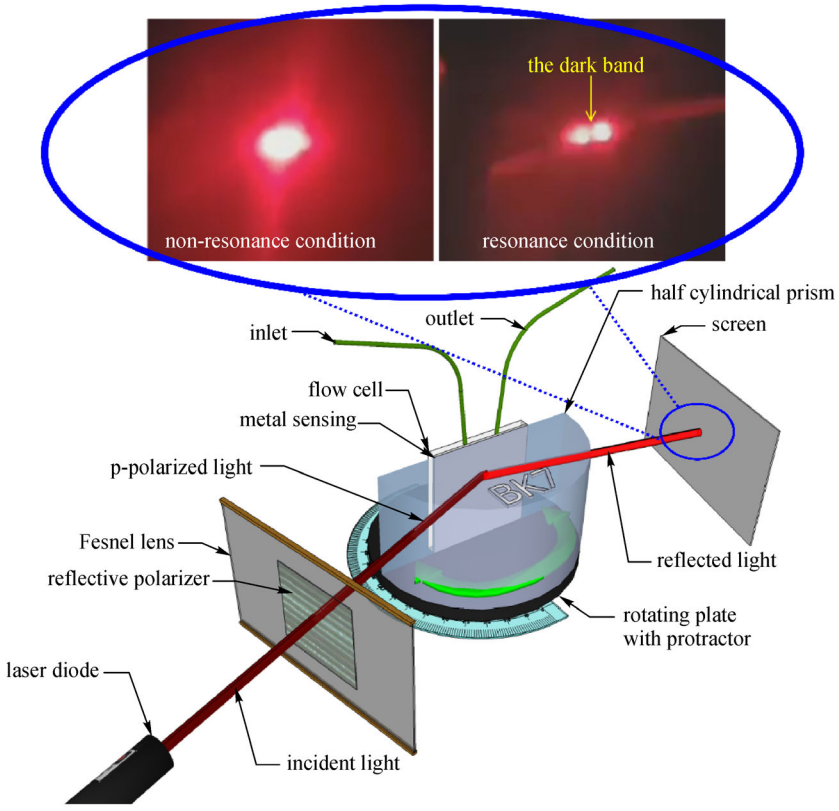

Fig. 1 SPR sensor setup using a half cylindrical Kretschmann prism. An Al sensing layer protected by thin Au film was configured for a metal sensing structure of the SPR sensor

2.2 Experimental setup

The platform was constructed using half cylindrical BK7 prism with a diameter of 80 mm (HiLite Optronics Inc., Hsinchu, Taiwan, China). For the optical convergence, the collimating lens was using a Fresnel lens with a focal length of 5.08 cm (Edmund Optics Inc., New Jersey, USA). The polarizer film using DBEF (3M, Minnesota, USA) was attached in the Fresnel lens and a rotating plate with the angular scale (Chief SI Co., Hsinchu, Taiwan, China). The light source used for the whole experiment was a red laser diode (WelTek Co. Ltd., Taoyuan, Taiwan, China). The metallic sensing layer was deposited by thermal evaporation deposition with a very low deposition rate (0.5 Å/s) in vacuum pressure below 1×10^{-6} Torr. The polydimethylsiloxane (PDMS) flow cell was a homemade design using molding techniques and constructed with peristaltic tubes (Gilson, Middleton, USA). The peristaltic pump (Shishin Tech., Taipei, Taiwan, China) was utilized to flow the liquid samples. The refractive indices sample was prepared by sucrose (Sigma Aldrich, Missouri, USA) diluted in deionized (DI) water by weight percentage to obtain particular refractive index values. The sucrose water concentrations were 0, 18, 34.8, 45.1, 54.6, 63.5 wt%, which corresponded to the refractive index (RI) value 1.33, 1.36, 1.39, 1.41, 1.43, and 1.45 RIU, respectively.

3 Results and discussion

The following equation describes the wave vector of the surface plasmon (K_{SP}) along the interface (x-direction) [44]:

$$K_{SP} = \frac{2\pi}{\lambda}\sqrt{\frac{\varepsilon_M \varepsilon_D}{\varepsilon_M + \varepsilon_D}}, \quad (1)$$

where λ is the wavelength of the incident light, ε_M and ε_D are real parts of the dielectric constant of the metallic sensing layer and medium, respectively. If we consider the Drude model [45] where the ε_M of the thin film metal is a negative value, there is a possibility that the value of K_{SP} is imaginary when $|\varepsilon_M| < \varepsilon_D$. In this condition, surface plasmon wave in the metal-dielectric interface does not exist. Thus, only several metals have potential properties to generate surface plasmon. In addition, in the case of too high dielectric constant value of the medium, the K_{SP} value will be imaginary as well. In this case, the resonance condition is limited in a particular point of the refractive index (or dielectric constant) of the medium. In the sensing technology perspective, this point is the dynamic range limit of the sensing performance.

While in Kretschmann-based SPR configuration, the resonance condition can be obtained when the incident light in particular angle (θ) through high refractive index

prism excites the metal sensing as described by

$$\sin\theta = \frac{1}{n_{\mathrm{P}}}\sqrt{\frac{\varepsilon_{\mathrm{M}}\varepsilon_{\mathrm{D}}}{\varepsilon_{\mathrm{M}}+\varepsilon_{\mathrm{D}}}}, \tag{2}$$

where n_{p} is the refractive index value of the prism.

As the resonance condition is reached, the reflectivity curve can be seen in the reflectance light profile along the incident angle axis. The reflectivity of the attenuated total reflectance (ATR) through high refractive index prism around the resonance angle can be explained by [46]

$$R = |r_{\mathrm{pmd}}|^2, \tag{3}$$

where

$$r_{\mathrm{pmd}} = \frac{r_{\mathrm{pm}} + r_{\mathrm{md}}\exp(2ik_{\mathrm{mx}}t)}{1 + r_{\mathrm{pm}}r_{\mathrm{md}}\exp(2ik_{\mathrm{mx}}t)}, \tag{4}$$

where t is the metallic sensing layer thickness, and

$$k_{ix} = \sqrt{\left(\frac{2\pi}{\lambda}\right)^2 \varepsilon i - k_z^2}, \tag{5}$$

and for the p-polarized light:

$$r_{ij} = \frac{\varepsilon_j\varepsilon_{ix} - \varepsilon_i k_{jx}}{\varepsilon_j k_{ix} + \varepsilon_i k_{jx}}, \tag{6}$$

where the subscripts i and j are p, m, or d indicating for prism, metal, and dielectric, respectively.

The reflectivity profile of the Al sensing layer compared to the other noble metals, such as Au and Ag, is demonstrated in Fig. 2(a). In 600 nm wavelength light, based on McPeak et al.'s report [41], the $\varepsilon_{\mathrm{Mreal}}$ value for Au, Ag, and Al are −10.47, −16.34, and −39.58, respectively. The substantial negative value of Al $\varepsilon_{\mathrm{Mreal}}$ is an exciting property to be utilized for sensing layer in SPR sensor; in contrast, Al also exhibits high k-value of 6.36 while Au is 3.24 and Ag is 4.04, This property is responsible for the light absorption significantly.

For further detail analysis, the penetration depth (d) of the evanescent wave inside the medium or metal by each of metal structure can be calculated by

$$d = \frac{1}{K_{yi}}, \tag{7}$$

where K_{yi} is the surface plasmon wave vector in the y-direction described by

$$K_{yi} = \frac{2\pi}{\lambda}\sqrt{\frac{\varepsilon_i^2}{\varepsilon_{\mathrm{M}}\varepsilon_{\mathrm{D}}}}, \tag{8}$$

where ε_i can be ε_{M} or ε_{D} for the penetration inside the metal or medium, respectively. From Eq. (4) when K_{SP} value in Eq. (1) is real, the K_{yi} value will be imaginary due to $|\varepsilon_{\mathrm{M}}| > \varepsilon_{\mathrm{D}}$. This mathematical approach indicates that the evanescent wave exponentially decays in its penetration into the medium or metal (inset Fig. 2(b)) [47]. The calculated penetration depth inside the medium and metals, where $|\varepsilon_{\mathrm{M}}|$ is taken into Eq. (4) were plotted in Fig. 2(b). From this analytical calculation, Al performed the deepest penetration inside the measured medium around 346 nm in 600 nm of wavelength in comparison with the penetration depth of Au (188 nm) and Ag (229 nm), respectively.

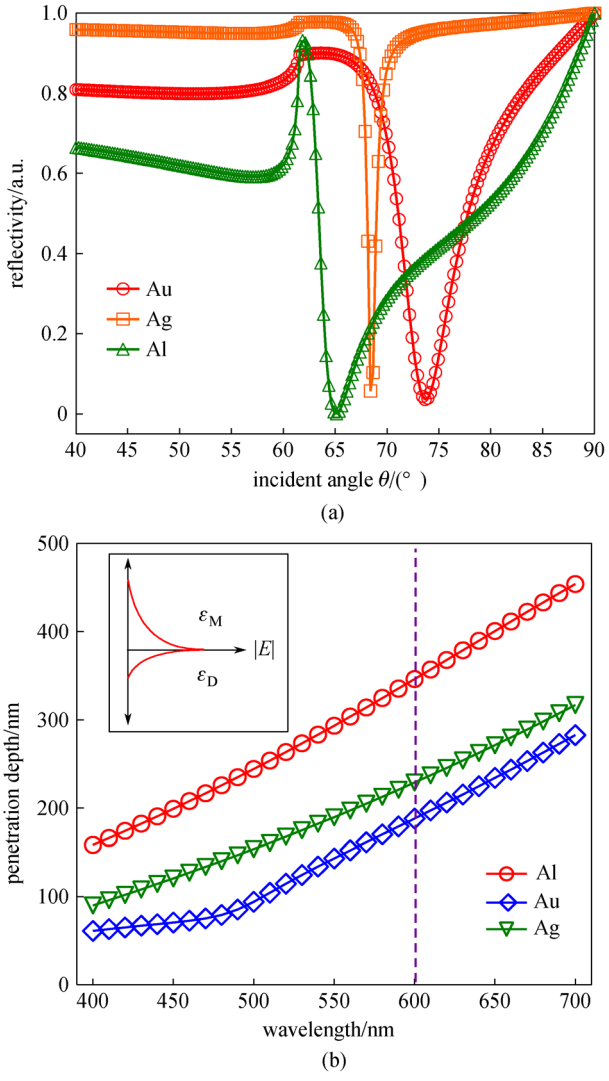

Fig. 2 (a) SPR reflectivity profile of monolayer Au, Ag, and Al, coupling by BK7 prism and water for the dielectric medium; (b) calculated penetration depth of evanescent wave inside the medium by several metals around the visible range. The dashed line is the 600 nm of wavelength penetration depth in this study. Inset is the evanescent wave profile representing the penetration depth from the interface of a metal and dielectric medium

In the results displayed in Figs. 2(a) and 2(b), water as the dielectric medium is taken into account. As postulated in Eqs. (1) and (2), the dielectric constant of the medium ($\varepsilon_{\mathrm{Dreal}}$) is the predominant factor for surface plasmon generation besides the dielectric constant of the metal

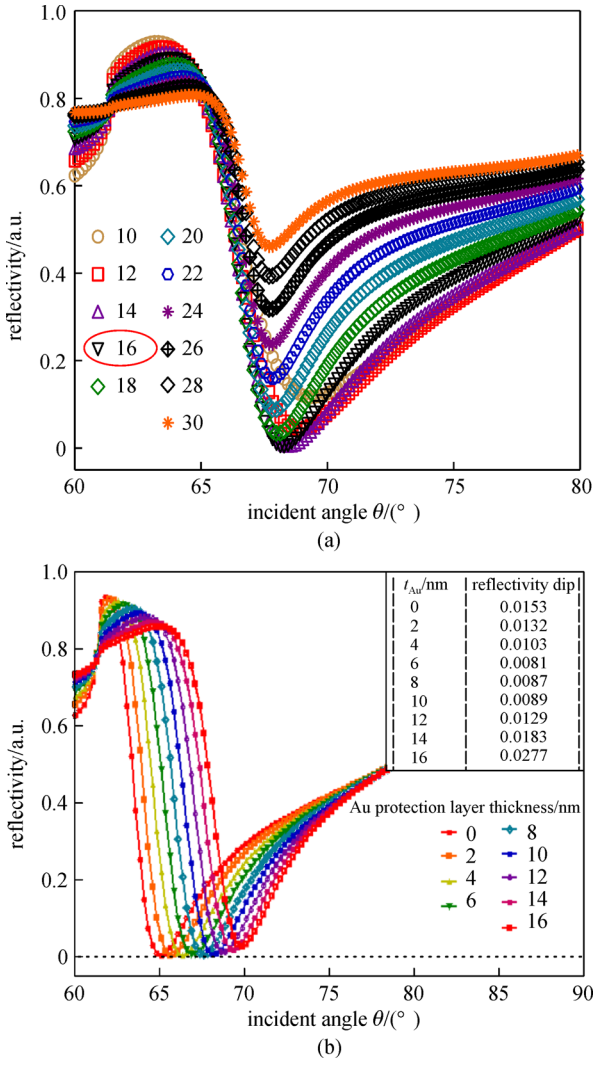

Fig. 3 Optimization of (a) Al thickness (unit in nm) covered by 10 nm of Au, and (b) Au protection layer thickness with 16 nm of Al sensing layer. Inset shows the minimum point of the reflectivity profile of each Au thickness

(ε_{Mreal}). Consequently, in the case of the different refractive index value of the medium, the penetration depth could be different due to the different wave vector of surface plasmon wave. Therefore, in this analytical study, as the application is dedicated to the water and environmental monitoring, the water as the medium of the basic analytical and design is applied.

The optimization of aluminum layer thickness in the SPR configuration is presented in Fig. 3(a) where the optimum reflectivity dip was obtained at the thickness of 16 nm. In addition, as a protection layer, the Au thickness optimization was simulated from 0 to 16 nm with 2 nm of step as shown in Fig. 3(b). The minimum reflectivity dip values are demonstrated in the inset of Fig. 3(b). Interestingly, the Au protection layer thickness up to 16 nm insignificantly changes the value of minimum reflectivity dip as presented in the inset. The standard deviation of the minimum reflectivity dip was about 0.58% calculated. However, in the real manufacturing process, the formation of Au film below 8 nm is not yet naturally constructed. In this condition, the Au material tends to form nano-islands morphology [48–51]. With this fundamental finding, a 10 nm of Au protection layer was carried out throughout the further analytical study.

The simulated measurement of a series of the solution with different bulk refractive index values was plotted in Fig. 4. The SPR reflectivity shifted from lower to higher resonance angle as the refractive index solution increased (Fig. 4(a)). The correlation of n and k of the medium to the ε_D can be expressed by

$$\varepsilon_D = n_D^2 - k_D^2, \tag{9}$$

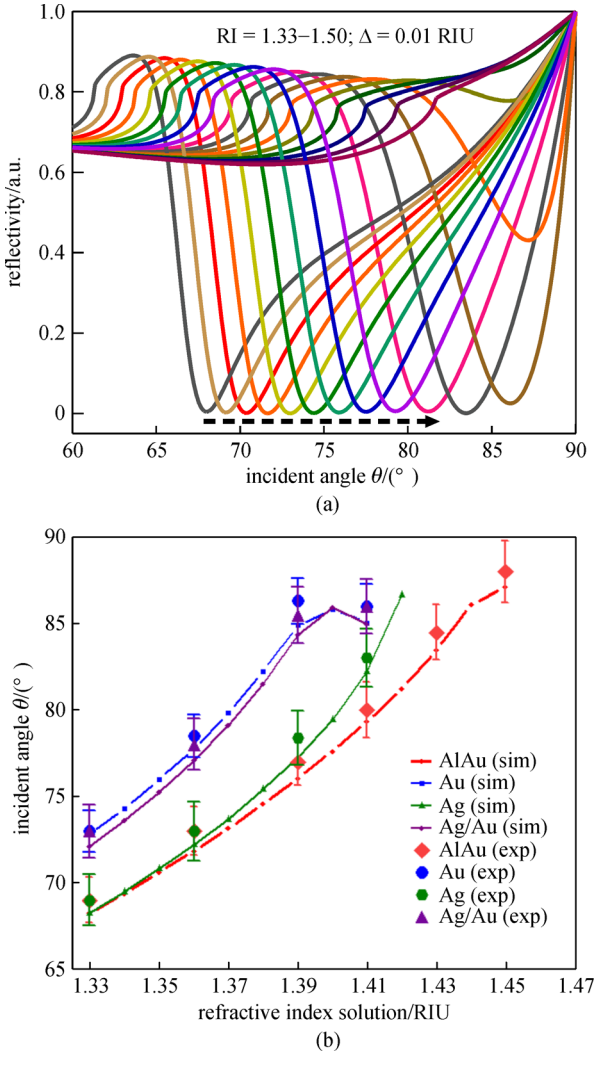

Fig. 4 Proposed metallic sensing layer response to the samples with various refractive index values. (a) Reflectivity dip shifting; (b) detection response and its range of the proposed sensing layers compared to other sensing structures

where n_D and k_D are refractive index and extinction coefficient of the medium, respectively. Moreover, when the refractive index solution escalated, the ε_D exponentially increased, and the resonance angle as described in Eq. (2) shifted to the higher incident angle. Finally, with the refractive index value above 1.45, the resonance of surface plasmon did not occur. This dynamic range of Al/Au sensing is highly superior as compared to other sensing structures, such as Au, Ag, or bimetallic Ag/Au as presented in Fig. 4(b).

The experimental work demonstrated the proof-of-concept of the proposed sensing platform with optical configuration for the various measurement of RI samples prepared by sucrose-water solution (Fig. 1). First, the laser diode was passed through the Fresnel lens [52] to maintain the collimation of the laser beam. The flat geometry of Fresnel lens has an advantage that the reflective polarizer film [37] can be attached in the smooth surface of the lens to obtain the p-polarized light as the primary mechanism to couple the SPR. Later, the laser beam was passed through the half cylindrical prism to avoid the refraction phenomena due to the air and prism interface. The sensing metals were located in the center origin of the prism geometry, and the PDMS fluidic cell was attached to flow the sample. The PDMS chamber was designed in the center origin of the prism as well. The total internal reflection (TIR) of the laser beam was observed on the screen. The measurements were done by flowing the measured sample then rotating the protractor plate until the dark band appeared in the laser spot on the screen (see supplementary material video). The presence of the dark band indicates that the SPR condition has been obtained and the protractor angle position is recorded. The results were plotted in Fig. 4 which confirms a good agreement with the simulation results.

In the case of anisotropic surface refractive index solution [46], the simulation results were shown in Fig. 5. Anisotropic surface refractive index solution is a typical case for the target sample diluted in buffer. This scenario mostly happens in the bio-detection instances. For example, when antibodies are diluted in the phosphate buffer saline (PBS), the immobilized antibodies near the metal surface give a slightly higher n compared to the n of solution buffer with the assumption that the thickness of the IgG antibody and its antigen are around 28 – 30 nm [53], respectively. The assumption of 60 nm of the surface refractive index around the metal sensing was configured. As the results, the potential dynamic range of the sensing performance in this anisotropic measurement was prominently improved to 1.58 RIU. Nonetheless, the sensitivity performance implies a trade-off in the lower slope of resonance angle response compared to the bulk refractive index measurement. As a matter of fact, in the bio-detection, a sensitivity performance is more valuable than that of the dynamic range. Based on this analysis, this sensing structure is more suitable for measurement in the environment monitoring application, such as for high bulk refractive index sample like in oil contamination control.

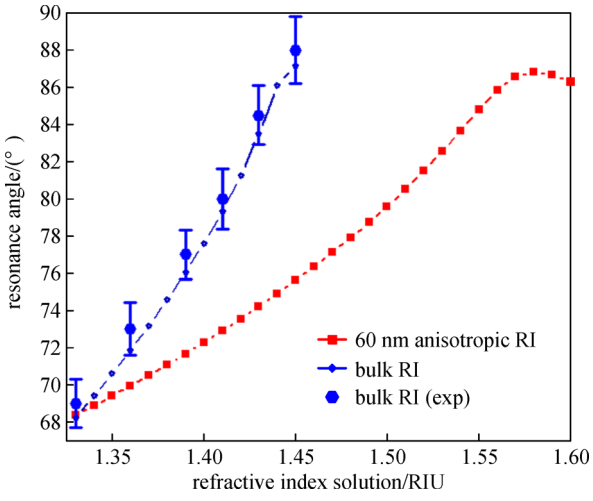

Fig. 5 Detection response and its theoretical range of the anisotropic refractive index sample measurement compared to the bulk refractive index samples

Finally, the summary of related work of dynamic range performance in SPR sensor platform is presented in Table 1. It is revealed that the dynamic range performance

Table 1 Summary of dynamic range performance from related SPR sensor development

No.	technical remarks	dynamic range limit[a)]	Ref.
1	fiber-optic-based SPR sensor	up to 1.4018 RIU (correspond to 6.98×10^{-2} RIU)	[54]
2	long range SPR sensor	8×10^{-3} RIU	[55]
3	two channels fiber-optic-based SPR sensor	up to 1.385 TIU (correspond to 5.3×10^{-2} RIU)	[56]
4	multi-channel SPR sensor based on single-mode and multimode optical fiber	up to 1.385 RIU (correspond to 5.3×10^{-2} RIU)	[57]
5	reflective-distributed SPR sensor based on twin-core optical fiber	up to 1.385 RIU (correspond to 5.3×10^{-2} RIU)	[58]
6	distributed fiber SPR sensor	up to 1.385 RIU (correspond to 5.3×10^{-2} RIU)	[59]
7	wavelength interrogation, SPR imaging	4.63×10^{-2} RIU	[60]
8	SPR sensor based on injection-molded prism	0.1 RIU	[61]
9	SPR sensor based on phase interrogation	0.5 RIU	[62]
10	aluminum gold sensing on Kretschmann	up to 1.45 RIU (corresponded to 11.8×10^{-2} RIU)	this work

Note: a) For bulk refractive indice measurement with H_2O for baseline

of the proposed platform is comparable to the previously published reports.

4 Conclusion

A comprehensive characterization of Al/Au-based SPR sensing is analytically demonstrated and followed up by the proof-of-concept results experimentally. The detection range up to 1.45 RIU for bulk refractive index measurement was achieved. This high value of bulk refractive index solution is comparable to the 63.5 wt% of sucrose water concentration and 22% benzene on methanol solution. While for the anisotropic refractive index solution in the thickness of 60 nm, the detection range reached up to 1.58 RIU. From this study, we proposed the Al-based sensing platform for ultra-high dynamic range SPR sensor for environmental applications requiring high refractive index analyte, for example, in salt water monitoring, oil contamination study, or other high refractive indices fluidic measurement.

Acknowledgements This research was funded in part by Ministry of Science and Technology (MOST) (Taiwan, China) under the contract number of MOST 107-2218-E-182-008 and MOST 106-2221-E-182-041, also Chang Gung Memorial Hospital Grant with the contract number of CMRPDG0151. The authors thank the Indonesian Institute of Sciences and Chang Gung University for supporting this research. B.A.P. wholeheartedly thanks Chang Gung University, Taiwan, China for the visiting scholar invitation under the grant number BMRP741.

Electronic Supplementary Material Supplementary material is available in the online version of this article at https://doi.org/10.1007/s12200-019-0864-y and is accessible for authorized users.

References

1. Hoa X D, Kirk A G, Tabrizian M. Towards integrated and sensitive surface plasmon resonance biosensors: a review of recent progress. Biosensors & Bioelectronics, 2007, 23(2): 151–160
2. Linman M J, Abbas A, Cheng Q. Interface design and multiplexed analysis with surface plasmon resonance (SPR) spectroscopy and SPR imaging. Analyst (London), 2010, 135(11): 2759–2767
3. Homola J. Surface plasmon resonance sensors for detection of chemical and biological species. Chemical Reviews, 2008, 108(2): 462–493
4. Šípová H, Špringer T, Homola J. Streptavidin-enhanced assay for sensitive and specific detection of single nucleotide polymorphism in TP53. Analytical and Bioanalytical Chemistry, 2011, 399(7): 2343–2350
5. Prabowo B A, Chang Y F F, Lai H C C, Alom A, Pal P, Lee Y Y Y, Chiu N F F, Hatanaka K, Su L C C, Liu K C C. Rapid screening of mycobacterium tuberculosis complex (MTBC) in clinical samples by a modular portable biosensor. Sensors and Actuators B, Chemical, 2018, 254: 742–748
6. Prabowo B A, Wang R Y L, Secario M K, Ou P T, Alom A, Liu J J, Liu K C. Rapid detection and quantification of enterovirus 71 by a portable surface plasmon resonance biosensor. Biosensors & Bioelectronics, 2017, 92: 186–191
7. Zhao J, Cao S, Liao C, Wang Y, Wang G, Xu X, Fu C, Xu G, Lian J, Wang Y. Surface plasmon resonance refractive sensor based on silver-coated side-polished fiber. Sensors and Actuators B, Chemical, 2016, 230: 206–211
8. Gwon H R, Lee S H. Spectral and angular responses of surface plasmon resonance based on the Kretschmann prism configuration. Materials Transactions, 2010, 51(6): 1150–1155
9. Nguyen H H, Park J, Kang S, Kim M. Surface plasmon resonance: a versatile technique for biosensor applications. Sensors (Basel, Switzerland), 2015, 15(5): 10481–10510
10. Guo X. Surface plasmon resonance based biosensor technique: a review. Journal of Biophotonics, 2012, 5(7): 483–501
11. Chung J W, Bernhardt R, Pyun J C. Additive assay of cancer marker CA 19–9 by SPR biosensor. Sensors and Actuators B, Chemical, 2006, 118(1-2): 28–32
12. Averseng O, Hagège A, Taran F, Vidaud C. Surface plasmon resonance for rapid screening of uranyl affine proteins. Analytical Chemistry, 2010, 82(23): 9797–9802
13. Piliarik M, Párová L, Homola J. High-throughput SPR sensor for food safety. Biosensors & Bioelectronics, 2009, 24(5): 1399–1404
14. Zhang H, Yang L, Zhou B, Liu W, Ge J, Wu J, Wang Y, Wang P. Ultrasensitive and selective gold film-based detection of mercury (II) in tap water using a laser scanning confocal imaging-surface plasmon resonance system in real time. Biosensors & Bioelectronics, 2013, 47: 391–395
15. Prabowo B A, Alom A, Secario M K, Masim F C P, Lai H C, Hatanaka K, Liu K C. Graphene-based portable SPR sensor for the detection of mycobacterium tuberculosis DNA strain. Procedia Engineering, 2016, 168: 541–545
16. He Y J. Novel and high-performance LSPR biochemical fiber sensor. Sensors and Actuators B, Chemical, 2015, 206: 212–219
17. Mock J J, Hill R T, Tsai Y J, Chilkoti A, Smith D R. Probing dynamically tunable localized surface plasmon resonances of film-coupled nanoparticles by evanescent wave excitation. Nano Letters, 2012, 12(4): 1757–1764
18. Zhang J, Sun Y, Wu Q, Gao Y, Zhang H, Bai Y, Song D. Preparation of graphene oxide-based surface plasmon resonance biosensor with Au bipyramid nanoparticles as sensitivity enhancer. Colloids and Surfaces. B, Biointerfaces, 2014, 116: 211–218
19. Wu L, Chu H S, Koh W S, Li E P. Highly sensitive graphene biosensors based on surface plasmon resonance. Optics Express, 2010, 18(14): 14395–14400
20. Maurya J B, Prajapati Y K, Singh V, Saini J P. Sensitivity enhancement of surface plasmon resonance sensor based on graphene–MoS2 hybrid structure with TiO_2-SiO_2 composite layer. Applied Physics A, Materials Science & Processing, 2015, 121(2): 525–533
21. Zeng S, Hu S, Xia J, Anderson T, Dinh X Q, Meng X M, Coquet P, Yong K T. Graphene-MoS_2 hybrid nanostructures enhanced surface plasmon resonance biosensors. Sensors and Actuators B, Chemical, 2015, 207: 801–810
22. Piliarik M, Vala M, Tichý I, Homola J. Compact and low-cost biosensor based on novel approach to spectroscopy of surface plasmons. Biosensors & Bioelectronics, 2009, 24(12): 3430–3435

23. Prabowo B A, Alom A, Pal P, Secario M K, Wang R Y L, Liu K C. Novel four layer metal sensing in portable SPR sensor platform for viral particles quantification. Proceedings of Eurosensors, 2017, 1 (4): 528
24. Prabowo B A, Liu K C. Multi-metallic sensing layers for surface plasmon resonance sensor. In: Proceedings of IEEE SCOReD. Putrajaya: IEEE, 2017
25. Choi Y H, Lee G Y, Ko H, Chang Y W, Kang M J, Pyun J C. Development of SPR biosensor for the detection of human hepatitis B virus using plasma-treated parylene-N film. Biosensors & Bioelectronics, 2014, 56: 286–294
26. Szunerits S, Maalouli N, Wijaya E, Vilcot J P, Boukherroub R. Recent advances in the development of graphene-based surface plasmon resonance (SPR) interfaces. Analytical and Bioanalytical Chemistry, 2013, 405(5): 1435–1443
27. Vaisocherová H, Ševců V, Adam P, Špačková B, Hegnerová K, de los Santos Pereira A, Rodriguez-Emmenegger C, Riedel T, Houska M, Brynda E, Homola J. Functionalized ultra-low fouling carboxy- and hydroxy-functional surface platforms: functionalization capacity, biorecognition capability and resistance to fouling from undiluted biological media. Biosensors & Bioelectronics, 2014, 51: 150–157
28. Sabouri A, Yetisen A K, Sadigzade R, Hassanin H, Essa K, Butt H. Three-dimensional microstructured lattices for oil sensing. Energy & Fuels, 2017, 31(3): 2524–2529
29. Ramesh A K, Ramesh P. Trade-off between sensitivity and dynamic range in designing MEMS capacitive pressure sensor. In: Proceedings of IEEE TENCON. Macao: IEEE, 2016, 1–3
30. Dak P, Alam M A. Numerical and analytical modeling to determine performance tradeoffs in hydrogel-based pH sensors. IEEE Transactions on Electron Devices, 2016, 63(6): 2524–2530
31. Chen P, Shu X, Cao H, Sugden K. High-sensitivity and large-dynamic-range refractive index sensors employing weak composite Fabry-Perot cavities. Optics Letters, 2017, 42(16): 3145–3148
32. Prabowo B A, Purwidyantri A, Liu K C. Surface plasmon resonance optical sensor: a review on light source technology. Biosensors (Basel), 2018, 8(3): 80
33. Mishra A K, Mishra S K, Verma R K. An SPR-based sensor with an extremely large dynamic range of refractive index measurements in the visible region. Journal of Physics D, Applied Physics, 2015, 48 (43): 435502
34. Ong B H, Yuan X, Tan Y Y, Irawan R, Fang X, Zhang L, Tjin S C. Two-layered metallic film-induced surface plasmon polariton for fluorescence emission enhancement in on-chip waveguide. Lab on a Chip, 2007, 7(4): 506–512
35. Vandezande W, Janssen K P F, Delport F, Ameloot R, De Vos D E, Lammertyn J, Roeffaers M B J. Parts per million detection of alcohol vapors via metal organic framework functionalized surface plasmon resonance sensors. Analytical Chemistry, 2017, 89(8): 4480–4487
36. Greulich C, Braun D, Peetsch A, Diendorf J, Siebers B, Epple M, Köller M. The toxic effect of silver ions and silver nanoparticles towards bacteria and human cells occurs in the same concentration range. RSC Advances, 2012, 2(17): 6981–6987
37. Prabowo B A, Chang Y F, Lee Y Y, Su L C, Yu C J, Lin Y H, Chou C, Chiu N F, Lai H C, Liu K C. Application of an OLED integrated with BEF and giant birefringent optical (GBO) film in a SPR biosensor. Sensors and Actuators. B, Chemical, 2014, 198: 424–430
38. Abdelmalek F. Surface plasmon resonance based on Bragg gratings to test the durability of Au-Al films. Materials Letters, 2002, 57(1): 213–218
39. Jha R, Sharma A K. High-performance sensor based on surface plasmon resonance with chalcogenide prism and aluminum for detection in infrared. Optics Letters, 2009, 34(6): 749–751
40. Su L C, Chang C M, Tseng Y L, Chang Y F Y S, Li Y C, Chang Y S, Chou C. Rapid and highly sensitive method for influenza A (H1N1) virus detection. Analytical Chemistry, 2012, 84(9): 3914–3920
41. McPeak K M, Jayanti S V, Kress S J P, Meyer S, Iotti S, Rossinelli A, Norris D J. Plasmonic films can easily be better: rules and recipes. ACS Photonics, 2015, 2(3): 326–333
42. Hale G M, Querry M R. Optical constants of water in the 200-nm to 200-μm wavelength region. Applied Optics, 1973, 12(3): 555–563
43. Tan Y H, Liu M, Nolting B, Go J G, Gervay-Hague J, Liu G Y. A nanoengineering approach for investigation and regulation of protein immobilization. ACS Nano, 2008, 2(11): 2374–2384
44. Homola J J, Yee S S, Gauglitz G G. Surface plasmon resonance sensors. Sensors and Actuators B, Chemical, 1999, 54(1–2): 3–15
45. Li H Y, Zhou S M, Li J, Chen Y L, Wang S Y, Shen Z C, Chen L Y, Liu H, Zhang X X. Analysis of the drude model in metallic films. Applied Optics, 2001, 40(34): 6307–6311
46. Homola J. Surface Plasmon Resonance Based Sensors. Berlin: Springer, 2006
47. Kooyman R P H, Schasfoort R B M, Tudos A J. Physics of Surface Plasmon Resonance. In: Schasfoort R B M, Tudos A J, eds. Handbook of Surface Plasmon Resonance. Cambridge: The Royal Society of Chemistry, 2008, 403
48. Sun X, Li H. Gold nanoisland arrays by repeated deposition and post-deposition annealing for surface-enhanced Raman spectroscopy. Nanotechnology, 2013, 24(35): 355706
49. Kang M, Park S G, Jeong K H. Repeated solid-state dewetting of thin gold films for nanogap-rich plasmonic nanoislands. Scientific Reports, 2015, 5: 14790
50. Purwidyantri A, El-Mekki I, Lai C S. Tunable plasmonic SERS hotspots on Au-film over nanosphere by rapid thermal annealing. IEEE Transactions on Nanotechnology, 2017, 16(4): 551–559
51. Purwidyantri A, Kamajaya L, Chen C H, Luo J D, Chiou C C, Tian Y C, Lin C Y, Yang C M, Lai C S. A colloidal nanopatterning and downscaling of a highly periodic Au nanoporous EGFET biosensor. Journal of the Electrochemical Society, 2018, 165(4): H3170–H3177
52. Ullah I, Lv H, Whang A J W, Su Y. Analysis of a novel design of uniformly illumination for Fresnel lens-based optical fiber daylighting system. Energy and Building, 2017, 154: 19–29
53. Roberts C J, Williams P M, Davies J, Dawkes C, Sefton J, Edwards J C, Haymes G, Bestwick C, Davies M C, Tendler S J B. Real-space differentiation of IgG and IgM antibodies deposited on microtiter wells by scanning force microscopy. Langmuir, 1995, 11(5): 1822–1826
54. Kanso M, Cuenot S, Louarn G. Sensitivity of optical fiber sensor based on surface plasmon resonance: modeling and experiments. Plasmonics, 2008, 3(2-3): 49–57
55. Slavík R, Homola J. Optical multilayers for LED-based surface

plasmon resonance sensors. Applied Optics, 2006, 45(16): 3752–3759
56. Wei Y, Su Y, Liu C, Nie X, Liu Z, Zhang Y, Zhang Y. Two-channel SPR sensor combined application of polymer- and vitreous-clad optic fibers. Sensors (Basel, Switzerland), 2017, 17(12): 2862
57. Wei Y, Liu C, Zhang Y, Luo Y, Nie X, Liu Z, Zhang Y, Peng F, Zhou Z. Multi-channel SPR sensor based on the cascade application of the single-mode and multimode optical fiber. Optics Communications, 2017, 390: 82–87
58. Liu Z, Wei Y, Zhang Y, Zhu Z, Zhao E, Zhang Y, Yang J, Liu C, Yuan L. Reflective-distributed SPR sensor based on twin-core fiber. Optics Communications, 2016, 366: 107–111
59. Liu Z, Wei Y, Zhang Y, Liu C, Zhang Y, Zhao E, Yang J, Yuan L. Compact distributed fiber SPR sensor based on TDM and WDM technology. Optics Express, 2015, 23(18): 24004–24012
60. Zeng Y, Wang L, Wu S Y, He J, Qu J, Li X, Ho H P, Gu D, Gao B Z, Shao Y. Wavelength-scanning SPR imaging sensors based on an acousto-optic tunable filter and a white light laser. Sensors (Basel, Switzerland), 2017, 17(1): 90
61. Chen H, Chen C, Chang Y, Chuang H. Compact surface plasmon resonance biosensor utilizing an injection-molded prism. In: Proceedings of Advanced Environmental, Chemical, and Biological Sensing Technologies XIII. Baltimore: SPIE, 2018, 986205
62. Lan G, Liu S, Zhang X, Wang Y, Song Y. Highly sensitive and wide-dynamic-range liquid-prism surface plasmon resonance refractive index sensor based on the phase and angular interrogations. Chinese Optics Letters, 2016, 14(2): 022401–022405

Briliant Adhi PRABOWO received the Ph.D. degree from Department of Electronics Engineering, Chang Gung University, Taiwan, China. His research topics are related to the photonic sensor, organic electronic devices, bioelectronics, and biosensor. In addition, he received his Master of Engineering in Center for Computational Microelectronics, Department of Computer Science and Information Engineering Asia University, Taiwan, China. His master research was related to TCAD Engineering (2D and 3D) for power devices reliability include AlGaN/GaN HEMTs appliance, the bipolar transistor, and LDMOS. He received Bachelor Engineering from Soegijapranata Catholic University, Semarang, Indonesia in 2005. In April 2006, he joined PT. Televisi Transformasi Indonesia (Trans TV) in Transmission Department, and worked on satellite and microwave communication field for broadcasting. In January 2008, he joined Indonesian Institute of Sciences (LIPI) at Research Center for Informatics, and from 2017 he joins the Research Center for Electronics and Telecommunications. Recently he joins a visiting scholar program in Organic Electro-optical Device group, Chang Gung University, Taiwan, China.

I Dewa Putu HERMIDA completed his Master's degree at Bandung Institute of Technology (ITB), Bandung, in 2003. Currently, he works at the Indonesian Institute of Sciences (LIPI) from 1993, as Head of Analysis Circuit, at Research Center and Development TELKOMA-LIPI, 1998 – 2003, Head of Microelectronics Component, Research Center for Electronics and Telecommunications–LIPI, 2010 – 2013. The fields of research are sensors, microelectronics, and materials.

Robeth Viktoria MANURUNG studied biophotonics at Yang Ming University, Taiwan, China, and obtained his Ph.D. degree in 2016 with the topic of research "Nanostructured platform for biomedical implant and bioimaging." Currently, he works at Research Centre for Electronics & Telecommunication, Indonesian Institute of Sciences, Indonesia since 1996. His current research interests cover biosensor especially electrochemical biosensor, materials science at the nanoscale, with a particular focus on functional materials and up conversion nanoparticles processes for bioimaging and drug delivery. Several international publication have been produced as the output of his research expertise. Also he has recently organized The 2018 International Conference on Radar, Antenna, Microwave, Electronics and Telecommunications (ICRAMET) which is also technically sponsored by IEEE Indonesian Chapter.

Agnes PURWIDYANTRI received her Bachelor's degree in food technology from Soegijapranata University, Indonesia in 2007 and Master's degree in biotechnology from Asia University, Taiwan, China in 2013. Her Ph.D. was obtained from Chang Gung University in biomedical engineering, Taiwan, China in 2017. During her Ph.D. and postdoctoral programs, she joined the Semiconductor Laboratory, Biosensor Group at Chang Gung University under the supervisory of Prof. Chao-Sung Lai. She currently serves as a research fellow at the Research Unit for Clean Technology (LPTB), Indonesian Institute of Sciences (LIPI). Her interests comprise the development of multi-implementative nanostructure for biosensors, such as field-effect transistor, electrochemical sensor, surface-enhanced Raman spectroscopy (SERS) for biomedical application, green synthesized and biomaterial-based sensing platforms and environmental monitoring.

Kou-Chen LIU is the full professor and former chairperson of the Electronics Engineering Department, Chang Gung University, Taiwan, China. He is also affiliated to Division of Pediatric Infectious Disease, Department of Pediatrics, Chang Gung Memorial Hospital, and Department of Materials Engineering, Ming Chi University of Technology, Taiwan, China. He received the doctoral degree from the University of Texas at Austin, USA, Department of Electrical Engineering. In 2002 he joined the Graduate Institute of Optoelectronics, Chang Gung University, Taiwan, China, and receive the full professorship in Department of Electronics Engineering in 2012. His recent research interests are in the area of thin film transistor devices, organic electronics, polymer LED, and past years are focusing on the portable SPR biosensor for various biomedical applications. He received several top national research grants from Ministry of Science and Technology (Taiwan, China) for engineering and biosensor research, also from Chang Gung Memorial Hospital for clinical research and biosensor applications. He has several patents in thin-film technology and biosensing platform. He is a routine reviewer in several reputable international journals in the area of thin solid film, organic electronics and biosensor application fields. He has several year research experiences in Industrial Technology Research Institute (ITRI), Motorola, and the University of Texas-Austin. His past research works are related to ASIC design, deep development nano and submicron Si and SiGe vertical MOSFET, Si, SiGe Poly-TFT, SiGe, and SOI devices.